

Supporting Information

Drug-Drug Cocrystals of Anticancer Drugs Erlotinib-Furosemide and Gefitinib-Mefenamic acid for Alternative Multi-Drug Treatment

*Christy P. George,^a Shridhar H. Thorat,^{a,c} Parth S. Shaligram,^a P. R. Suresha,^b and Rajesh G. Gonnade^{*a,c}*

^aCenter for Materials Characterization, CSIR-National Chemical Laboratory, Pune - 411 008, India. *Fax:*

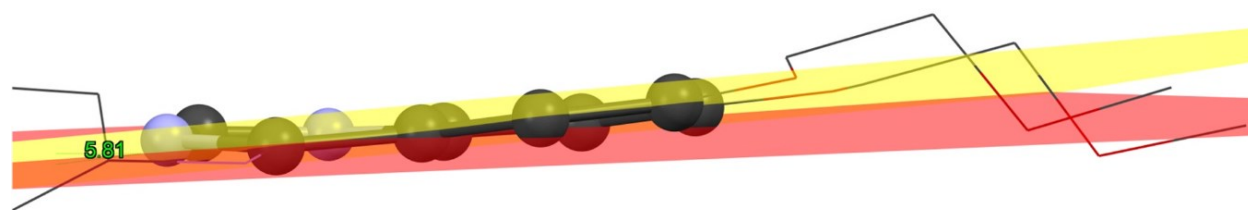
91-20-25902629; Tel: 91-20-25902055; E-mail: rg.gonnade@ncl.res.in

^bPolymer Science and Engineering Division, CSIR-National Chemical Laboratory, Pune - 411 008, India.

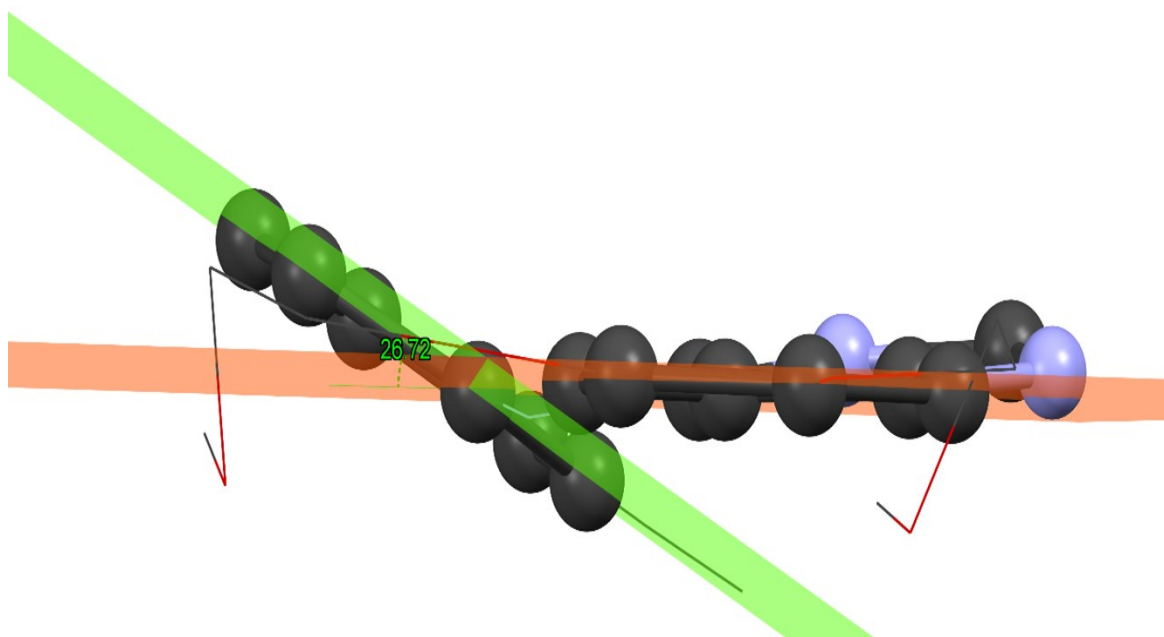
^cAcademy of Scientific and Innovative Research (AcSIR), Sector 19, Kamla Nehru Nagar, Ghaziabad, Uttar Pradesh 201002, India

	Content	Page
1	Figure S1. Conformational differences of different moieties of ETB.	4
2	Figure S2. A diagram showing the distortion of the N-H bond in the FSM molecule in the ETB-FSM cocrystal salt.	5
2	Figure S3. Conformational differences of different moieties of GTB.	6
4	Figure S4. A view of GTB-MFN cocrystal molecular packing down the c-axis	7
5	Figure S5. The overlay of the PXRD patterns of the ground samples of ETB and FSM.	8
6	Figure S6. The overlay of the PXRD patterns of the ground samples of GTB and MFN.	9
7	Figure S7. DSC profiles of ground samples of ETB and FSM	10
8	Figure S8. (a) DSC profiles of ground samples of GTB and MFN, (b) DSC profiles of GTB-MFN cocrystals heated up to 135 °C	11
9	Figure S9. Solubility data comparison at different pH conditions, a) ETB-HCL and ETB in ETB-FSM cocrystal b) FSM and FSM in ETB-FSM cocrystal.	12
10	Figure S10. The overlay of the PXRD profiles of the solid residue of ETB-FSM cocrystals at different pH conditions, ETB hydrochloride, ETB monohydrate and FSM.	13
11	Figure S11. Solubility data comparison at different pH conditions, a) GTB and GTB in GTB-MFN cocrystal b) MFN and MFN in GTB-MFN cocrystal.	14
12	Figure S12. The overlay of the PXRD profiles of the solid residue of GTB-MFN cocrystals at different pH conditions, GTB, GTB monohydrate and MFN.	15

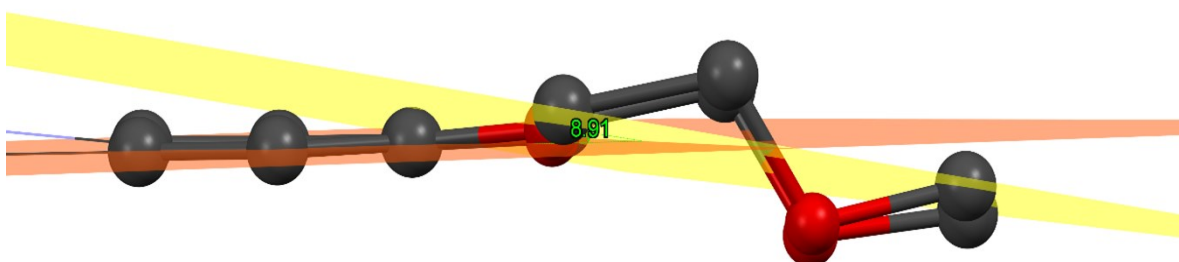
13	Figure S13. Molecular packing and intermolecular potentials energy values for ETB hydrochloride salt.	16
14	Figure S14. Molecular packing and intermolecular potentials energy values for ETB-FSM cocrystal.	17
15	Figure S15. Molecular packing and intermolecular potentials energy values for stable FSM polymorph.	18
16	Figure S16. Molecular packing and intermolecular potentials energy values for ETB-FSM cocrystal salt.	19
17	Figure S17. Molecular packing and intermolecular potentials energy values for GTB stable polymorph	20
18	Figure S18. A view of molecular packing down the c-axis and intermolecular potentials energy values for GTB stable polymorph	21
19	Figure S19. A view of molecular packing and intermolecular potentials energy values for GTB-MFN cocrystal	22
20	Figure S20. A view of molecular packing between the molecules of MFN in polymorph 1	23
21	Table S1: Solubility studies	24
22	Table S2: Dissolution data of ETB and FSM	25
23	Table S3: Dissolution data of GTB and MFN	26
24	Table S4: pH measurement studies before and after saturation	27



(a)



(b)



(c)

Figure S1. Conformational variances in different groups of ETB, (a) aromatic rings of quinazoline moiety, (b) phenyl ring of quinazoline moiety and ethynylbenzene and (c) phenyl ring of quinazoline moiety and dimethoxyethanes.

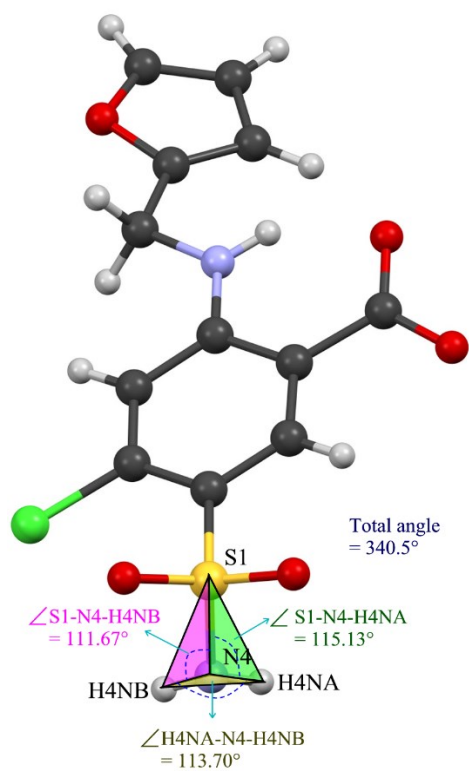


Figure S2. A diagram showing the distortion of the N-H bond in the FSM molecule in the ETB-FSM cocrystal salt.

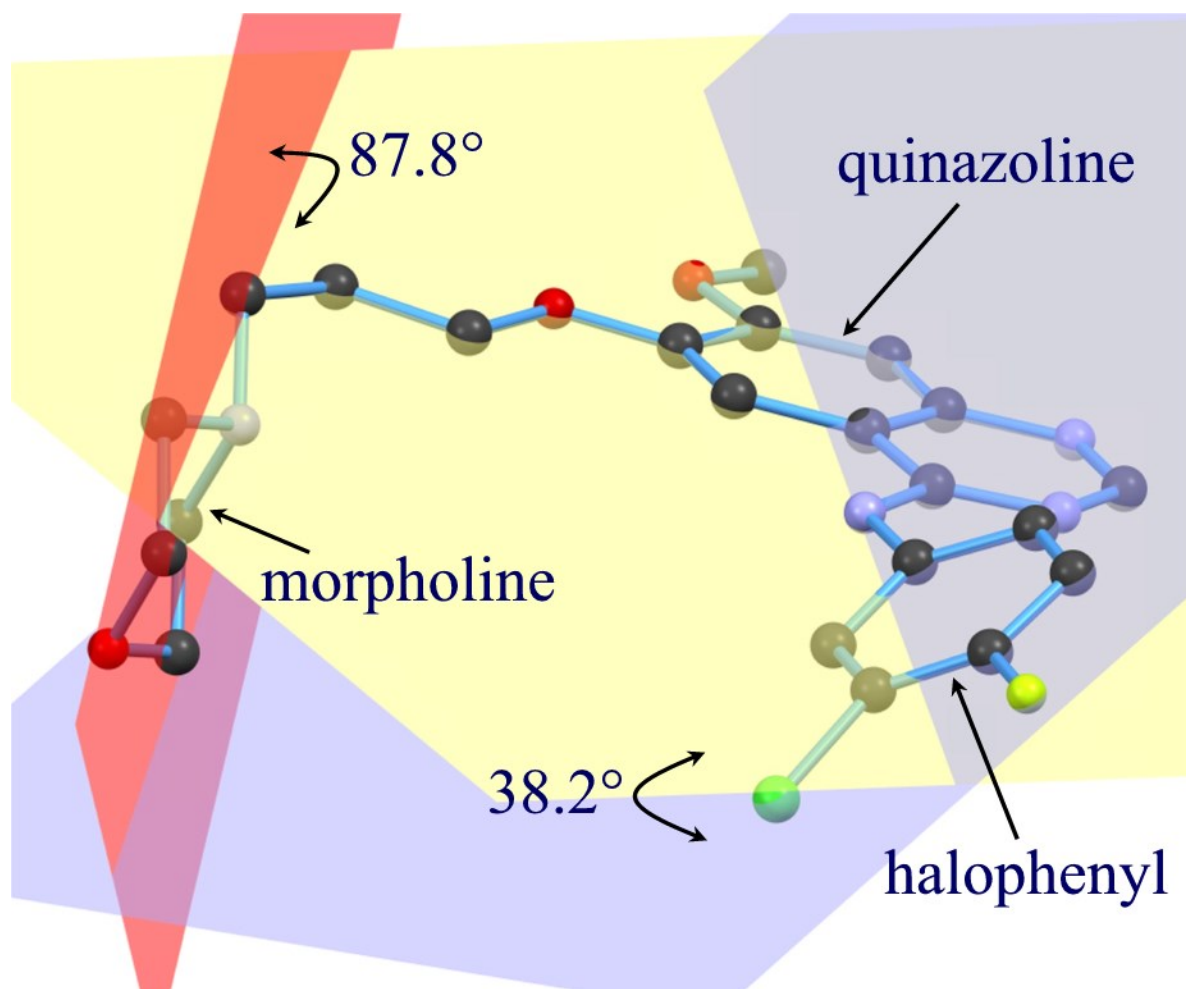


Figure S3. A diagram showing the conformational difference between quinazoline, morpholine and halophenyl moieties in GTB molecule of GTB-MFN cocrystal.

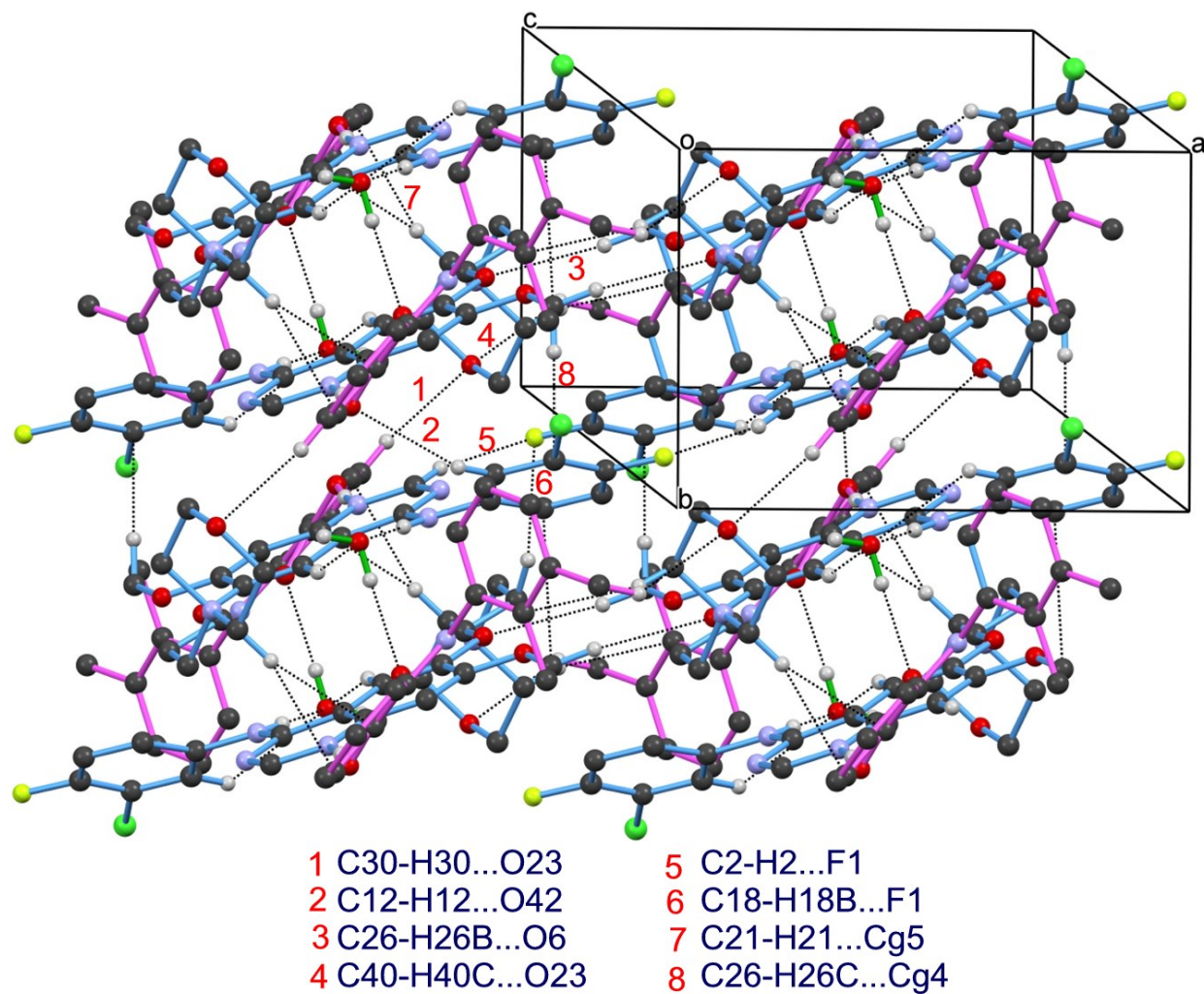


Figure S4. A view of molecular packing roughly down the c-axis showing a strong association between the molecules of GTB and MFN using C-H...O, C-H...F and C-H... π interactions.

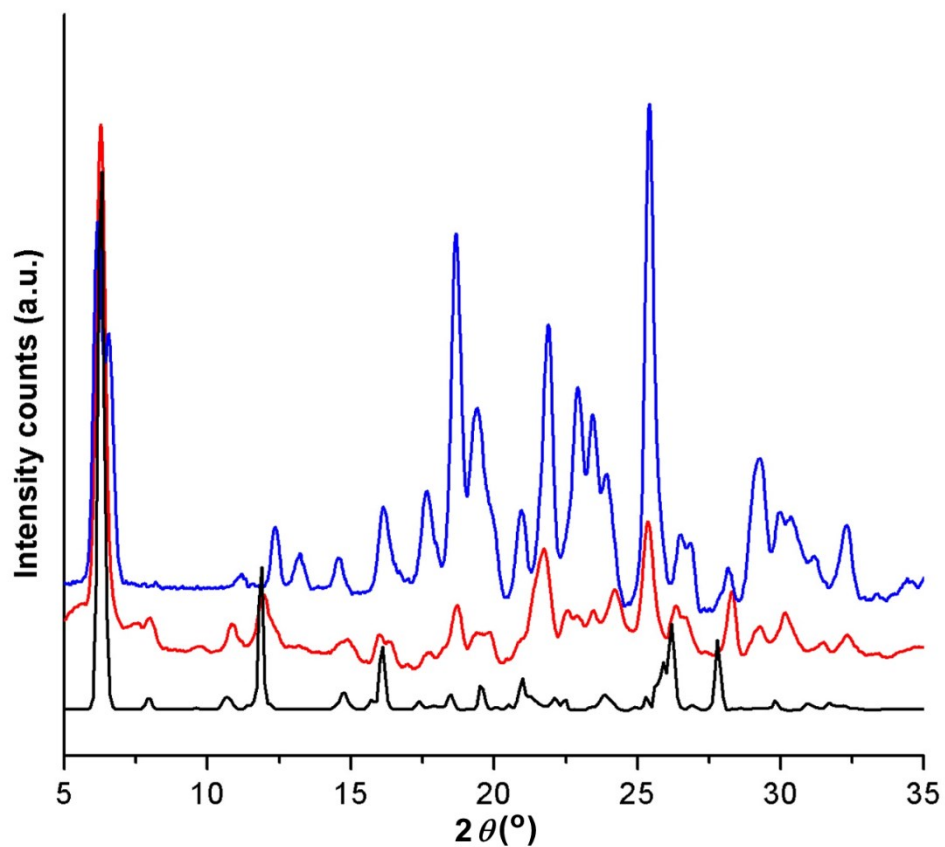


Figure S5. The overlay of the PXRD patterns of the ground samples of ETB and FSM (black, ETB-FSM obtained from solution crystallization; red, ETB-FSM obtained from liquid assisted grinding with n-butanol and blue, ETB-FSM obtained from dry grinding).

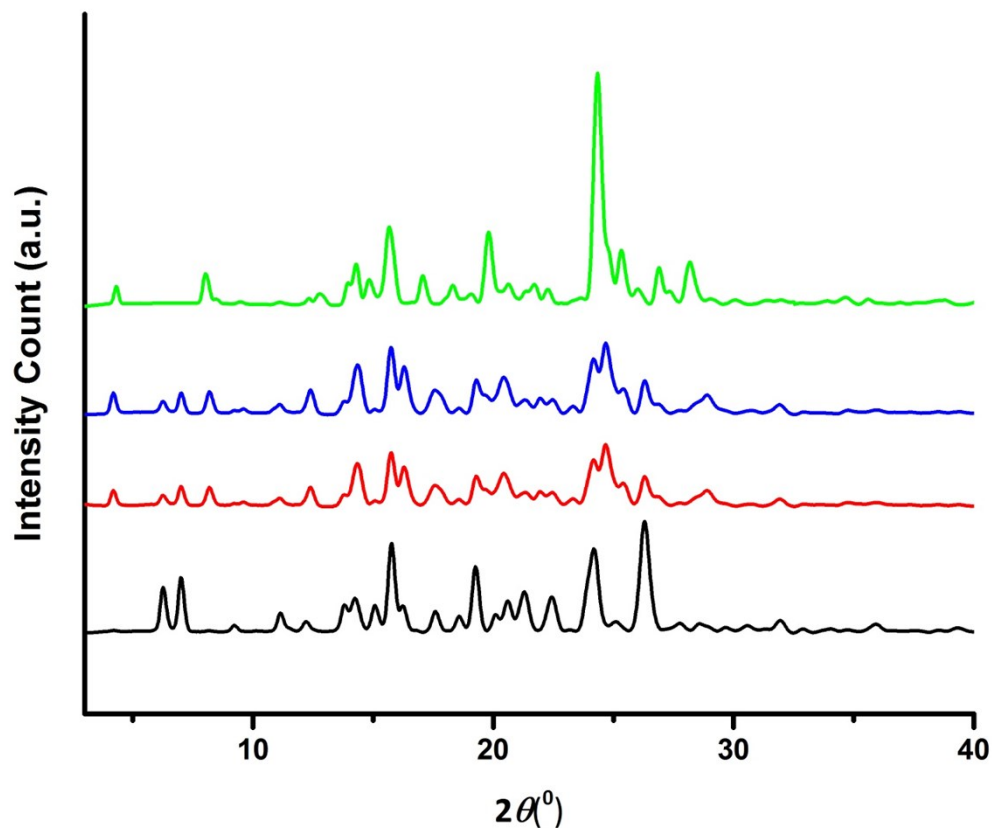
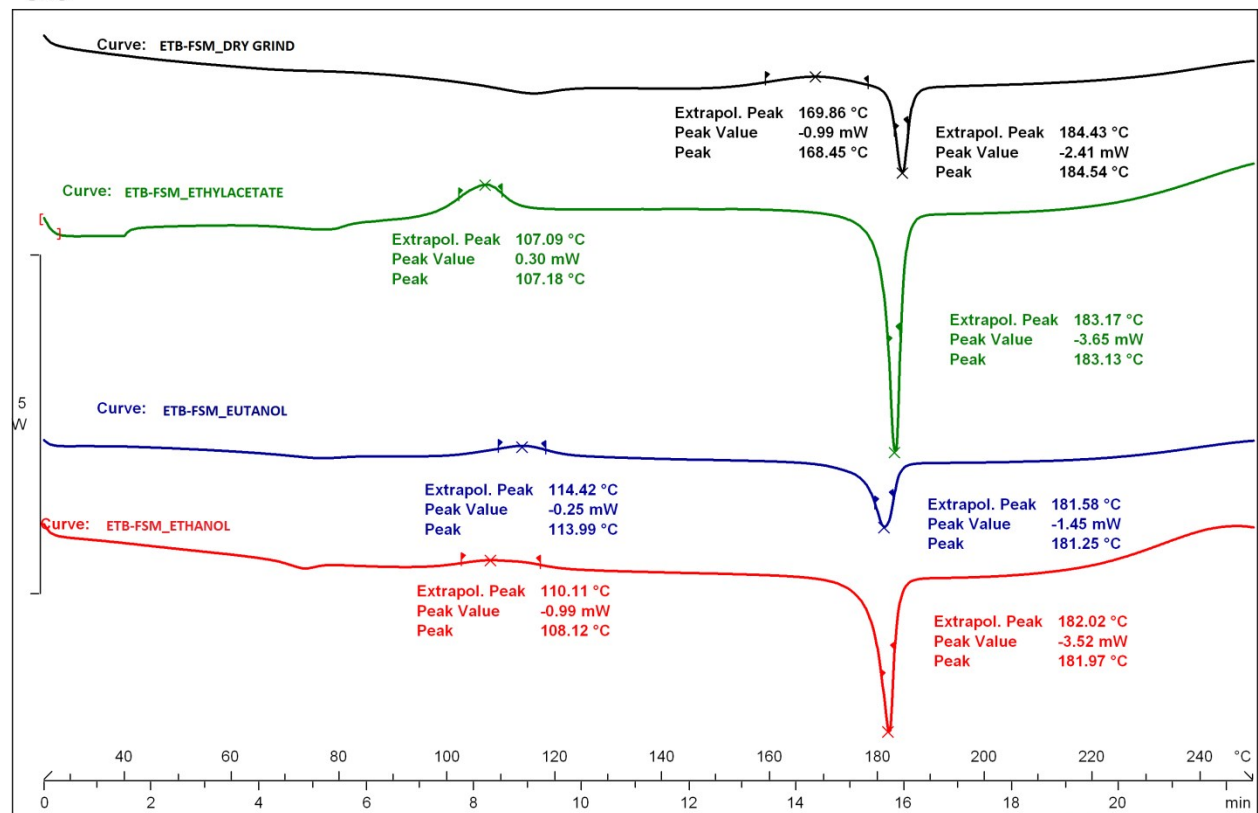


Figure S6. The overlay of the PXRD patterns of the ground samples of GTB and MFN; GTB-MFN cocrystal obtained from solution crystallization (green), GTB-MFN eutectic mixture obtained by dry grinding (blue), GTB-MFN eutectic mixture obtained by liquid assisted grinding using acetonitrile (red) and GTB-MFN eutectic mixture obtained by liquid assisted grinding using methanol (black).

^{exo}



Lab: METTLER

STAR^e SW 8.10

Figure S7. DSC profiles of ground samples of ETB and FSM; the dry grinding (black), wet grinding using ethyl acetate (green), wet grinding with *n*-butanol (blue) and wet grinding with ethanol (red).

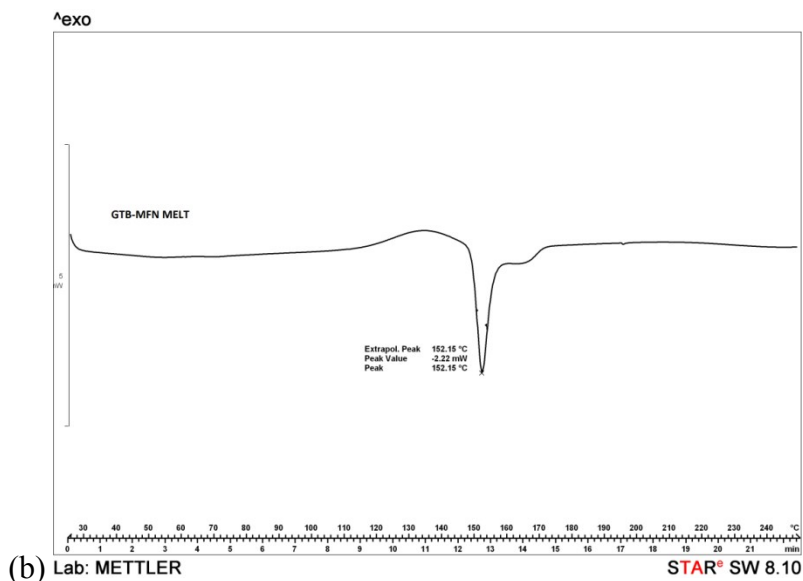
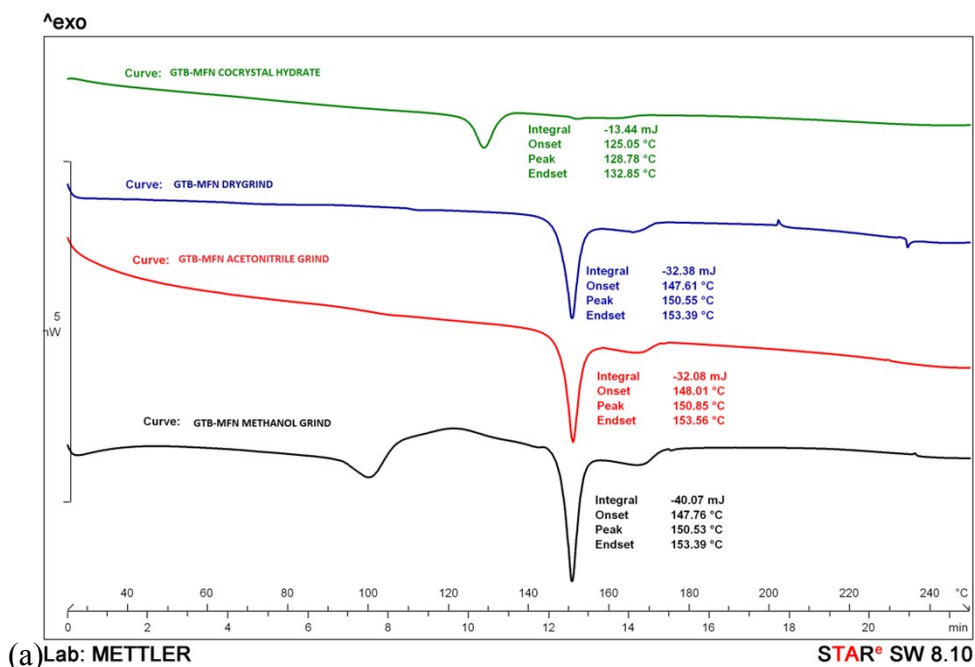


Figure S8. (a) DSC profiles of ground samples of GTB and MFN; GTB-MFN cocrystal obtained from solution crystallization (green), GTB-MFN eutectic obtained by dry grinding (blue), GTB-MFN eutectic obtained by liquid assisted grinding using n-acetonitrile (red), GTB-MFN eutectic obtained by liquid assisted grinding using methanol (black) and (b) DSC profile of the cooled (after heating up to 135 °C) solid residue of GTB-MFN cocrystal.

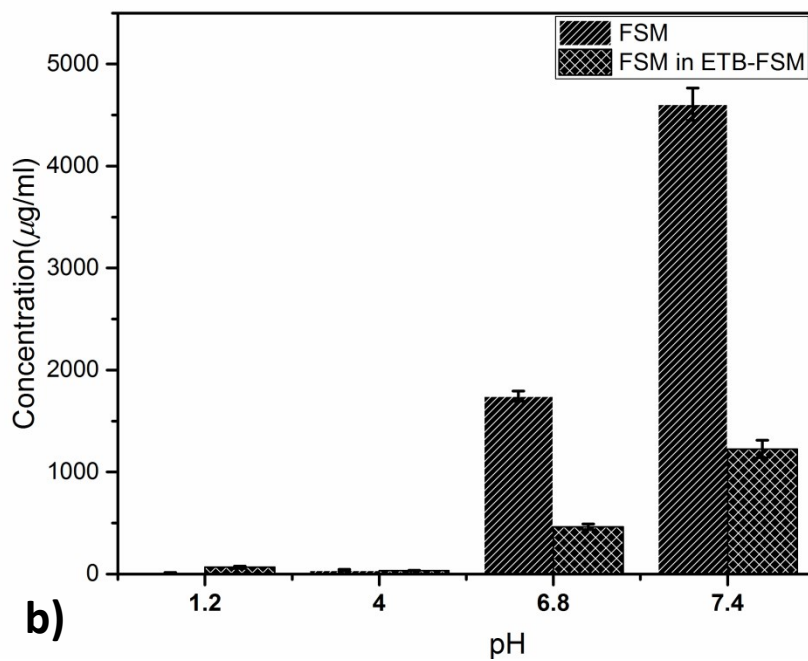
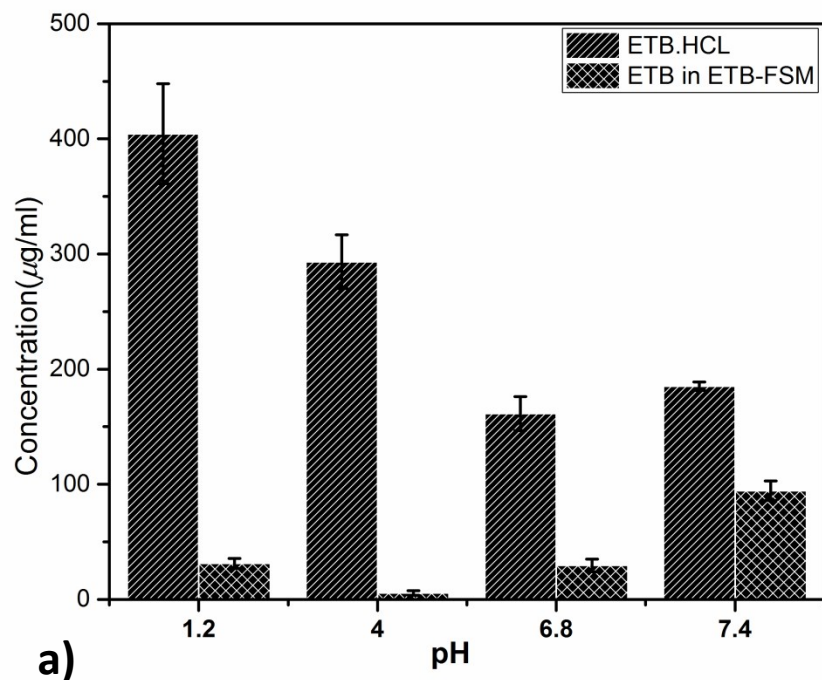


Figure S9. Solubility data comparison at different pH conditions, a) ETB-HCL and ETB in ETB-FSM cocystal b) FSM and FSM in ETB-FSM cocystal.

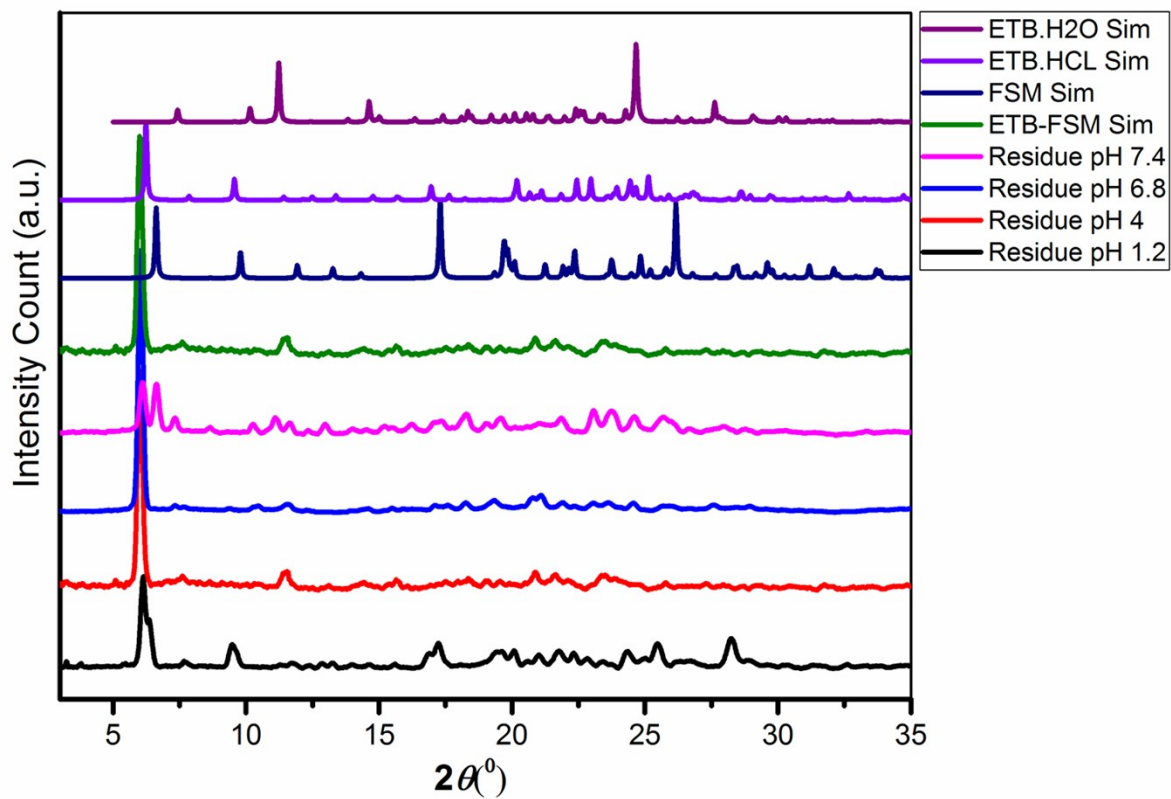


Figure S10. The overlay of the PXRD profiles of the solid residue of ETB-FSM cocrystals at different pH conditions, ETB hydrochloride, ETB monohydrate and FSM.

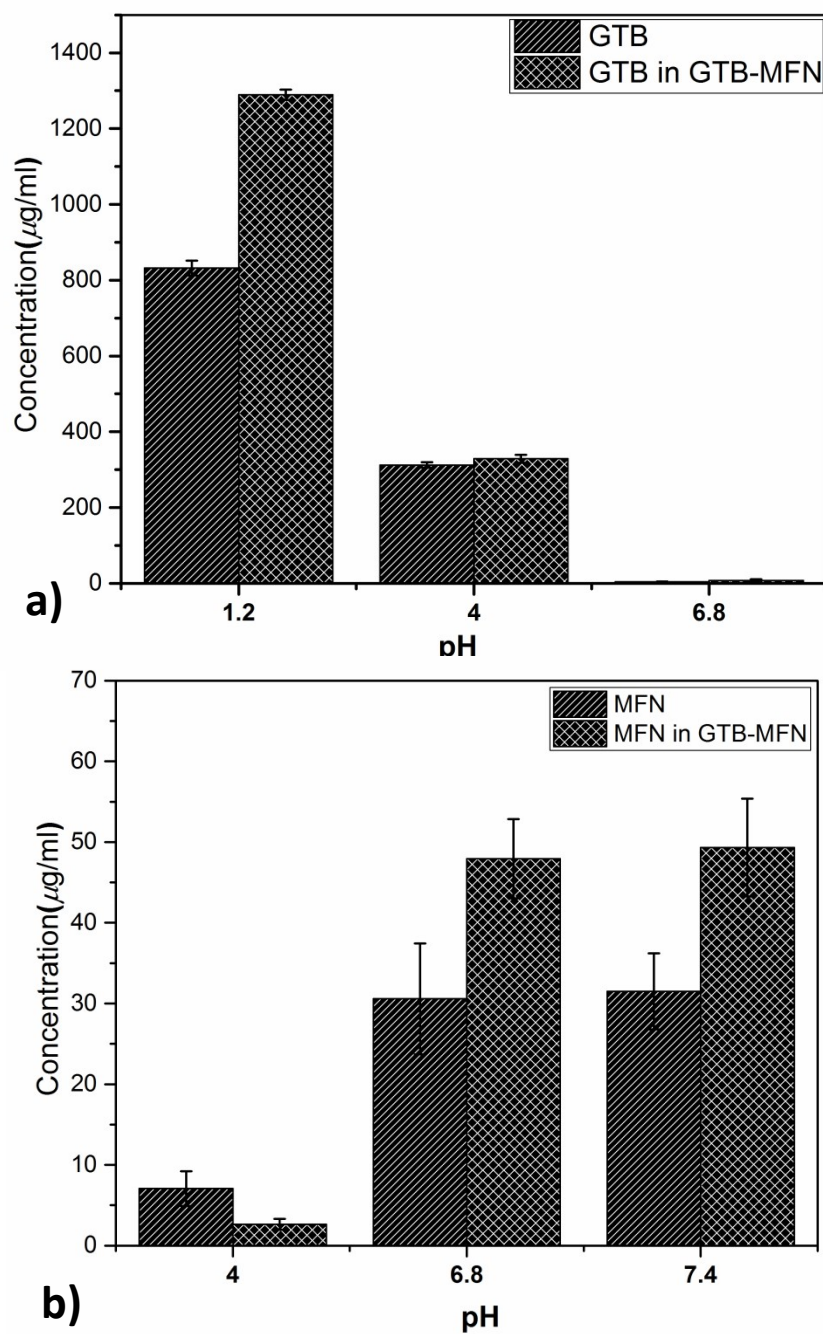


Figure S11. Solubility data comparison at different pH conditions, a) GTB and GTB in GTB-MFN cocrystal b) MFN and MFN in GTB-MFN cocrystal.

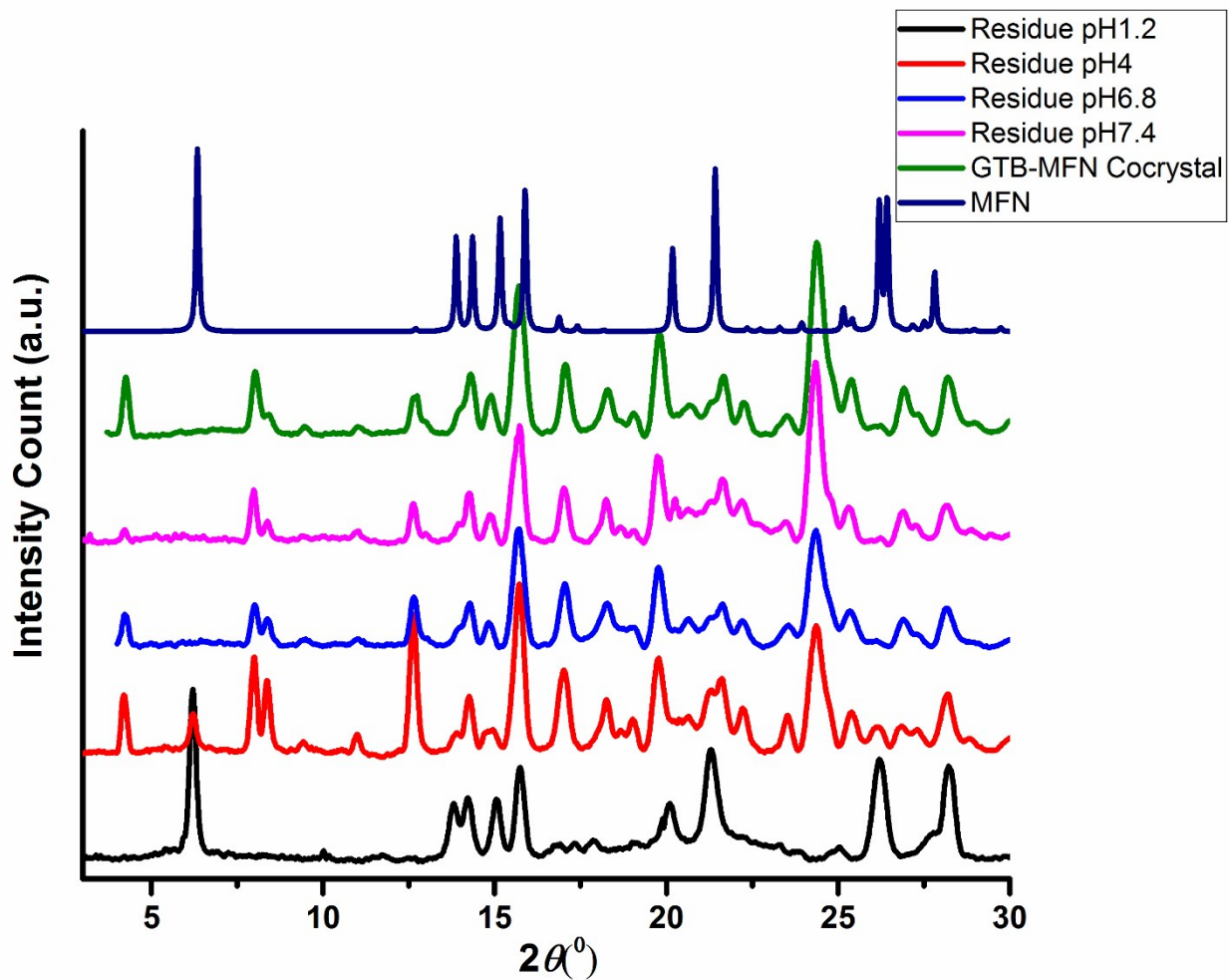


Figure S12. The overlay of the PXRD profiles of the solid residue of GTB-MFN cocrystals at different pH conditions, GTB, GTB monohydrate and MFN.

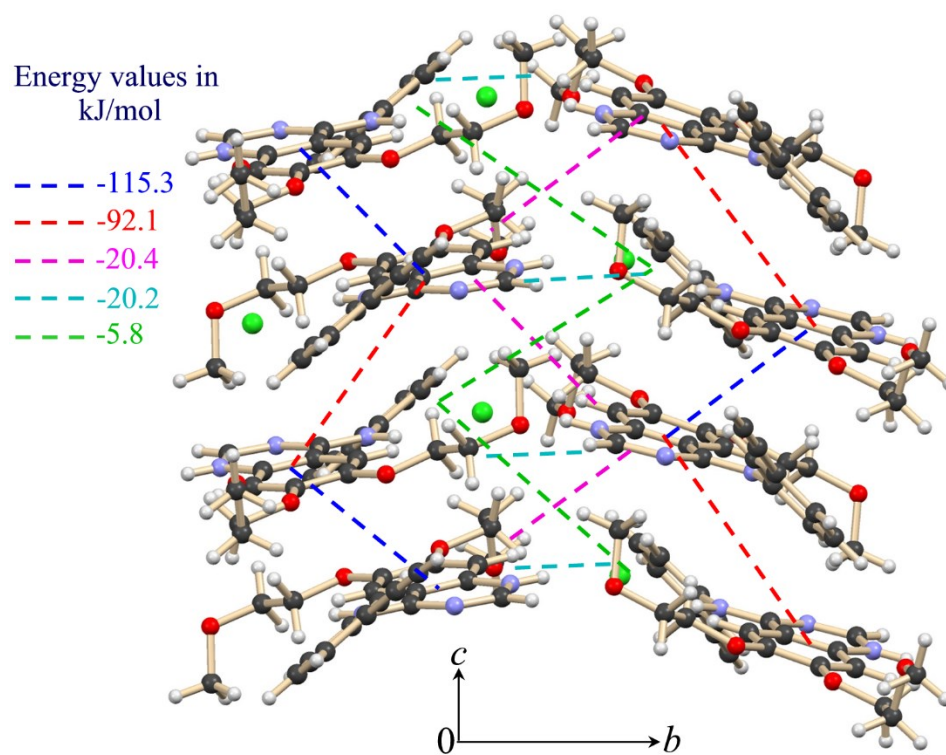


Figure S13. Molecular packing and intermolecular potentials energy values for ETB hydrochloride salt (the structure is retrieved from CSD, refcode: MIYBOM)

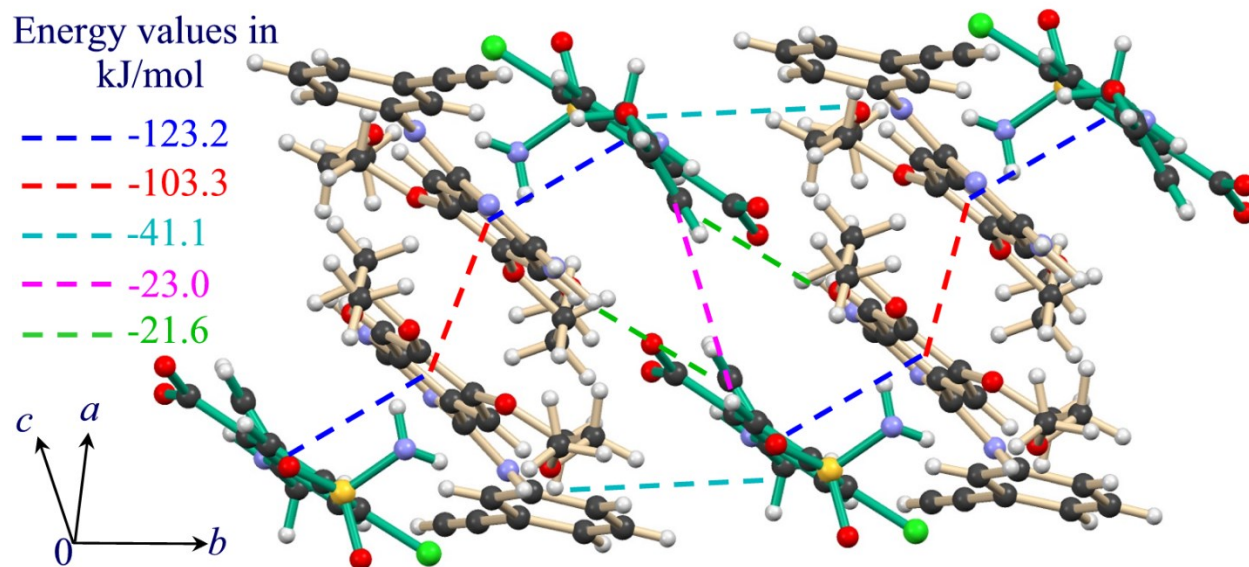


Figure S14. Molecular packing and intermolecular potentials energy values for ETB-FSM cocrystal.

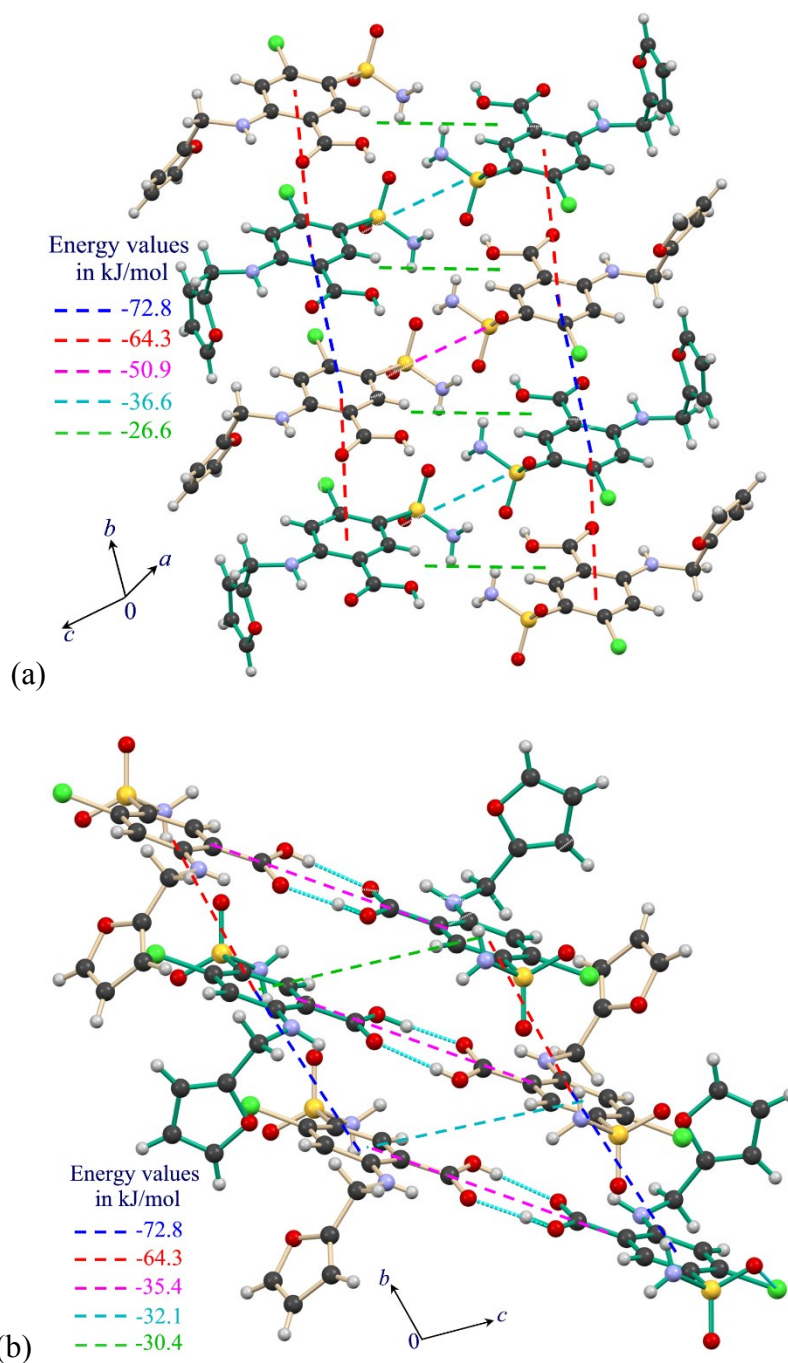


Figure S15. (a) and (b) Molecular packing and intermolecular potentials energy values for stable FSM polymorph (the structure is retrieved from CSD, Refcode: FURSEM13).

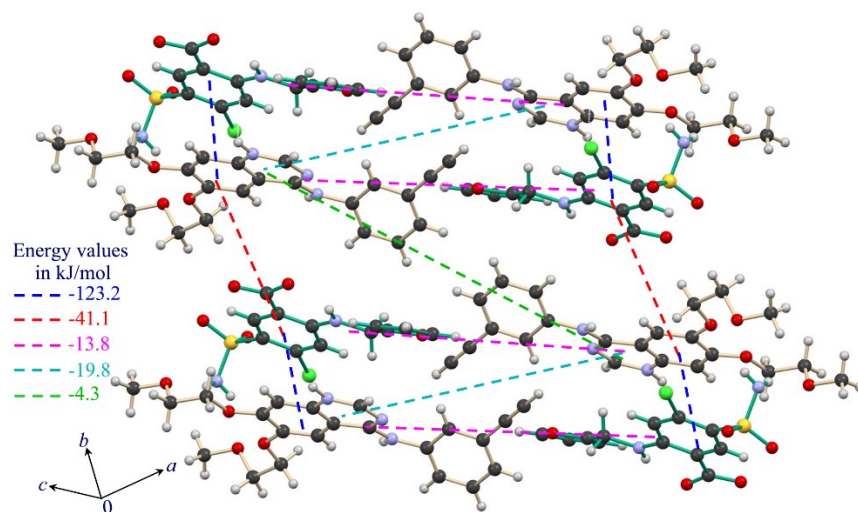


Figure S16. Molecular packing showing weak associations amongst the molecules of ETB and FSM roughly along the a-axis. The intermolecular potentials energy values are also depicted in the figure.

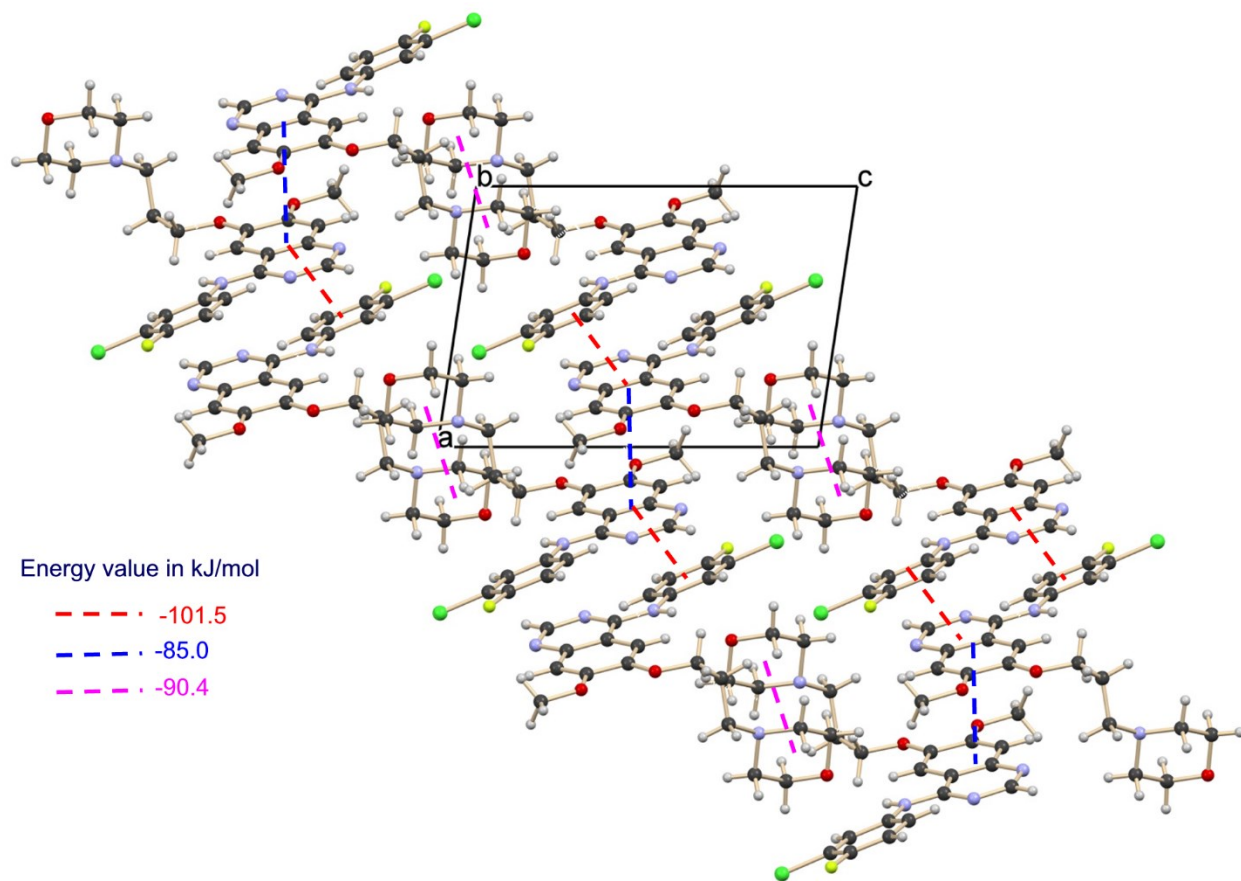


Figure S17. Molecular packing and intermolecular potentials energy values for GTB stable polymorph (the structure is retrieved from CSD, Refcode: FARRUM02).

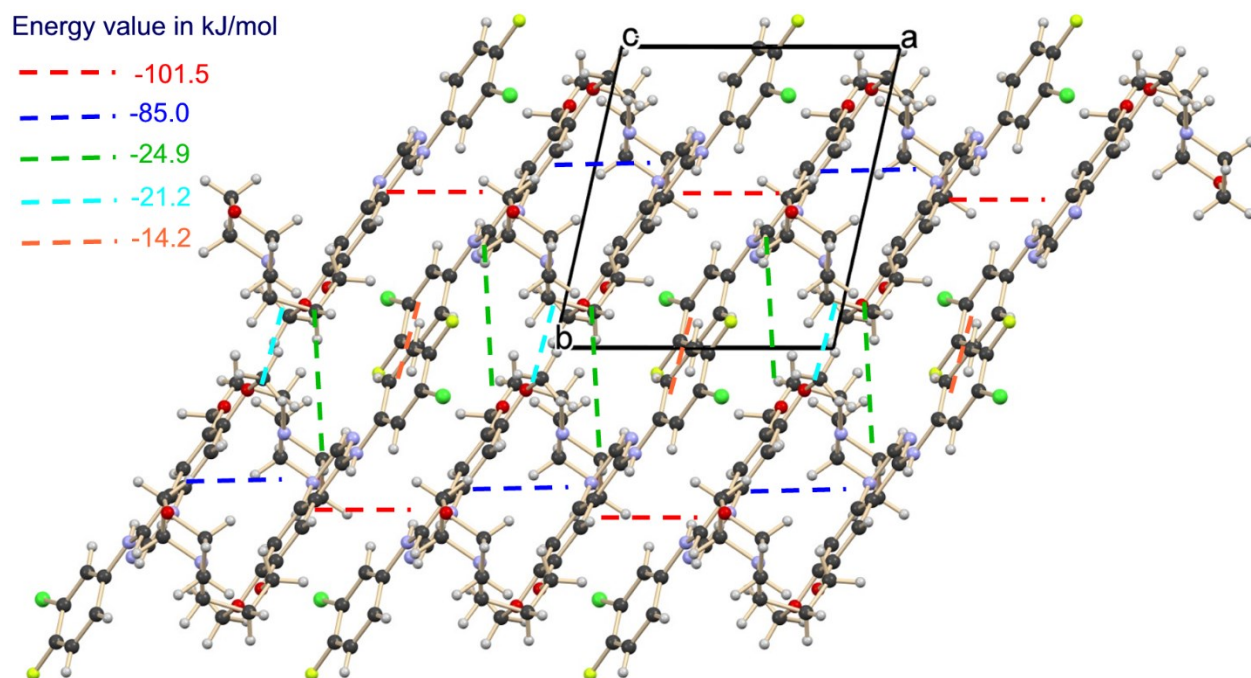


Figure S18. A view of molecular packing down the c-axis and intermolecular potentials energy values for GTB stable polymorph revealing loose linking of adjacent columns. (the structure is retrieved from CSD, Refcode: FARRUM02).

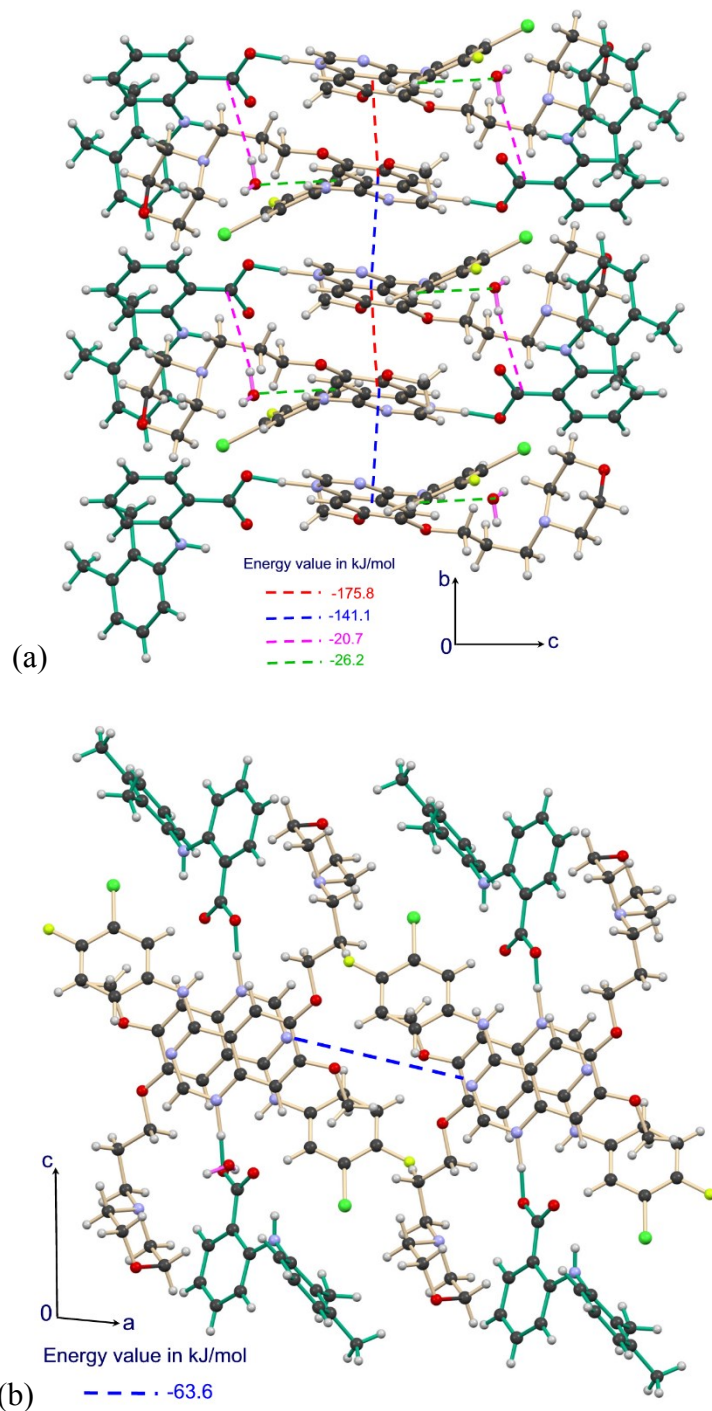


Figure S19. A view of molecular packing(a) down the a-axis and (b) down b-axis and intermolecular potentials energy values for GTB-MFN cocrystal revealing a strong association between the molecules of GTB using π -stacking and C-H...O interactions. While MFN molecules are loosely connected to GTB and water molecules using O-H...O hydrogen bonds compared to its polymorph I.

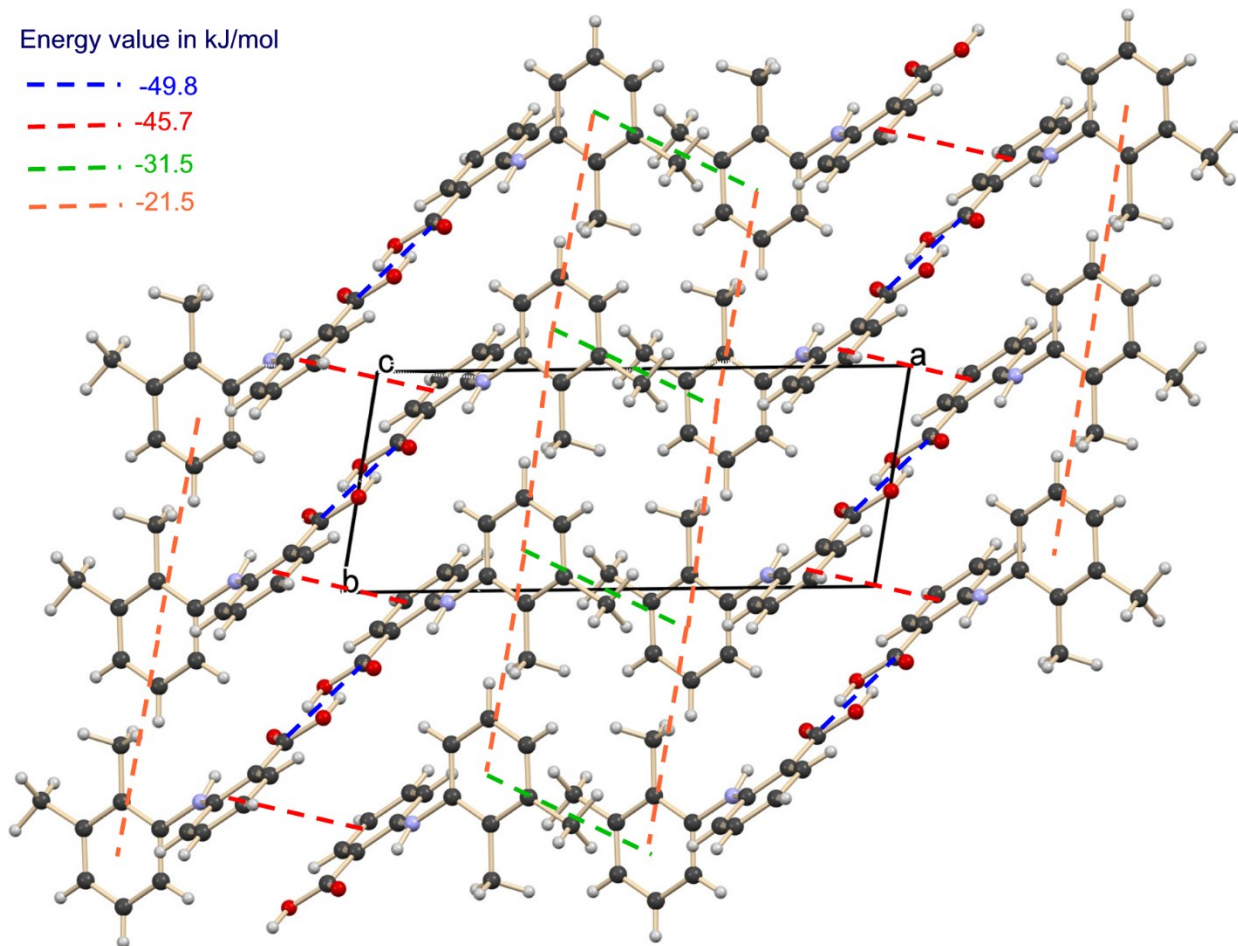


Figure S20. A view of molecular packing down the c-axis and intermolecular potentials energy values for MFN polymorph I revealing a strong association between the molecules of MFN using dimeric O-H...O hydrogen bonds, π -stacking and C-H... π interactions.

Table S1. Solubility data

pH	ETB-HCL conc($\mu\text{g}/\text{mL}$)	ETB in ETB-FSM conc($\mu\text{g}/\text{mL}$)	df	F Value	Prob>F	Significance
1.2	404.44 \pm 43.44	31.27 \pm 4.43	1,4	219.1403	1.21E-04	significant
4.2	293.33 \pm 23.36	5.67 \pm 2.03	1,4	451.4445	2.90E-05	significant
6.8	161.33 \pm 14.74	29.56 \pm 5.5	1,4	210.2221	1.32E-04	significant
7.4	185.11 \pm 3.67	94.44 \pm 8.53	1,4	103.3938	5.27E-04	significant
pH	FSM conc($\mu\text{g}/\text{mL}$)	FSM in ETB-FSM conc($\mu\text{g}/\text{mL}$)	df	F Value	Prob>F	Significance
1.2	14.47 \pm 1.04	66.83 \pm 10.3	1,4	76.76644	9.35E-04	significant
4.2	37.44 \pm 7.71	34 \pm 3.18	1,4	0.51165	0.51396	not significant
6.8	1743.33 \pm 50	463.06 \pm 26.79	1,4	1528.265	2.56E-06	significant
7.4	4605.56 \pm 158.4 1	1226.11 \pm 86.45	1,4	1052.085	5.39E-06	significant
pH	GTB conc($\mu\text{g}/\text{mL}$)	GTB in GTB-MFN conc($\mu\text{g}/\text{mL}$)	df	F Value	Prob>F	Significance
1.2	832.08 \pm 19.31	1289.52 \pm 13.35	1,4	1139.499	4.59E-06	significant
4.2	312.31 \pm 7.3	328.86 \pm 10.67	1,4	4.92168	0.09076	not significant
6.8	4.11 \pm 1.16	7.49 \pm 3.41	1,4	2.65591	0.1785	not significant
7.4	3.3 \pm 0.68	0 \pm 0		-	-	-
pH	MFN conc($\mu\text{g}/\text{mL}$)	MFN in GTB-MFN conc($\mu\text{g}/\text{mL}$)	df	F Value	Prob>F	Significance
1.2	2.54 \pm 1	0 \pm 0		-	-	-
4.2	7.06 \pm 2.16	2.65 \pm 0.66	1,4	11.49249	0.02753	significant
6.8	30.59 \pm 6.88	47.94 \pm 4.91	1,4	12.65052	0.02365	significant
7.4	31.5 \pm 4.71	49.32 \pm 6.07	1,4	16.13873	0.0159	significant

Data were statistically analyzed using Origin software using one way ANOVA ($p < 0.05$).

Table S2. Dissolution data of ETB and FSM

TIM E	ETB-HCL Conc. (µg/mL)	ETB in ETBFSM Conc. (µg/mL)	df	F Value	Prob>F	Significance
0	0±0	0±0		0	0	0
5	102.41±5.25	2.79±1.5	1,4	998.0254	5.98E-06	significant
10	165.78±4.54	5.04±1.56	1,4	3366.37	5.28E-07	significant
15	209.78±6.26	10.91±2.31	1,4	2659.666	8.46E-07	significant
20	237.51±5.01	8.12±3.72	1,4	4054.91	3.64E-07	significant
25	266.46±4.54	9.7±2.13	1,4	7879.922	9.65E-08	significant
30	281.25±8.18	10.79±3.2	1,4	2842.204	7.41E-07	significant
35	302.3±5.06	11.88±4.2	1,4	5855.684	1.75E-07	significant
40	324.31±4.58	12.8±2.5	1,4	10682.03	5.26E-08	significant
45	323.9±5.15	13.65±4	1,4	6784.009	1.30E-07	significant
50	342.34±6.11	14.45±3.56	1,4	6450.105	1.44E-07	significant
55	356.15±4.31	15.72±2.34	1,4	14462.84	2.87E-08	significant
60	371.08±7.86	16.47±3.92	1,4	4890.71	2.51E-07	significant
TIM E	FSM Conc. (µg/mL)	FSM in ETBFSM Conc. (µg/mL)	df	F Value	Prob>F	Significance
0	0±0	0±0		0	0	0
5	1.98±0.92	3.1±1.26	1,4	1.55094	2.81E-01	significant
10	1.55±0.83	5.26±2.78	1,4	4.89744	9.13E-02	significant
15	1.71±0.75	10.04±5.13	1,4	7.75132	4.96E-02	significant
20	1.94±0.9	8.72±2.75	1,4	16.41983	1.55E-02	significant
25	2.18±0.94	10.32±3.25	1,4	17.3092	1.41E-02	significant
30	2.87±0.64	11.28±2.75	1,4	26.52631	6.74E-03	significant
35	3.21±0.81	13.71±3.83	1,4	21.6009	9.68E-03	significant
40	3.38±0.81	14.05±3.3	1,4	29.48413	5.58E-03	significant
45	3.31±0.68	14.92±3.93	1,4	25.36958	7.30E-03	significant
50	3.62±0.68	16.41±4.97	1,4	19.5199	1.15E-02	significant
55	3.93±0.68	16.55±3	1,4	50.49951	2.07E-03	significant
60	4.12±0.68	19.68±6.81	1,4	15.51957	1.70E-02	significant

Data were statistically analyzed using Origin software using one way ANOVA (p<0.05).

Table S3. Dissolution data of GTB and MFN

TIME (min)	GTB Conc. (µg/mL)	GTB in GTB-MFN Conc. (µg/mL)	df	F Value	Prob>F	Significance
0	0±0	0±0		-	-	-
4	107.66±14.65	44.74±4.36	1,4	50.8663	0.00204	significant
10	94.61±6.64	77.86±3.31	1,4	15.26732	0.01743	significant
15	111.86±7.1	83.81±2.94	1,4	40.00711	0.0032	significant
20	116.98±6.64	104.4±3.71	1,4	8.2064	0.04571	significant
25	128.17±1.76	101.53±10.36	1,4	19.27211	0.01178	significant
30	129.8±10.38	109.25±3.01	1,4	10.85358	0.03009	significant
45	136.33±14.88	118.31±5.92	1,4	3.79454	0.12325	not significant
60	148.21±12.11	131.38±7.52	1,4	4.18246	0.1103	not significant
TIME (min)	MFN Conc. (µg/mL)	MFN in GTB-MFN Conc. (µg/mL)	df	F Value	Prob > F	Significance
0	0±0	0±0		-	-	-
4	0.07±0.02	0.58±0.05	1,4	256.8641	8.86E-05	significant
10	0.06±0.04	0.67±0.04	1,4	350.1641	4.80E-05	significant
15	0.13±0.02	0.74±0.03	1,4	972.0605	6.31E-06	significant
20	0.18±0.02	0.92±0.08	1,4	262.2208	8.51E-05	significant
25	0.2±0.02	0.88±0.06	1,4	405.6261	3.59E-05	significant
30	0.38±0.03	0.95±0.06	1,4	223.8323	1.16E-04	significant
45	0.45±0.02	1.23±0.26	1,4	26.9709	0.00655	significant
60	0.59±0.16	1.63±0.2	1,4	50.30863	0.00209	significant

Data were statistically analyzed using Origin software using one way ANOVA ($p < 0.05$). The dissolution rate measurement studies of GTB-MFN cocrystals were attempted in two different media, namely, HCl solution of **pH 3** (for GTB) and millipore water having **pH 6.9** (for MFN).

Table S4: pH measurement studies before and after saturation

Sr. No.	Initial pH	Final pH at 48 h (Control)	Final pH at 48h (ETB-FSM)	Diff. in pH	Final pH at 48 h (GTB-MFN)	Diff. in pH
1	1.22	1.41	1.25	0.16	1.28	0.13
2	4.01	4.32	4.37	-0.05	4.38	-0.06
3	6.79	6.92	6.95	-0.03	6.93	-0.01
4	7.39	7.4	7.41	-0.01	7.44	-0.04